Supplementary

Substituted naphtholates of rare earth metals as emissive materials

T. V. Balashova, N. A. Belova, M. E. Burin, D. M. Kuzyaev, R. V. Rumyantcev, G. K. Fukin, A. P. Pushkarev, V. A. Ilichev, A.F. Shestakov, I. D. Grishin, M. N. Bochkarev

Experimental

General Procedures

All experiments were performed in evacuated tubes using standard Schlenk techniques, thus excluding traces of air and water. Solvents (THF and DME) were purified by distillation from sodium/benzophenone ketyl. Silylamide complexes $Ln[N(SiMe_3)_2]_3$ (Ln = Sc, Nd, Gd, Er, Tm, Yb) were prepared according to the published procedure.[1] 3-(5-Methylbenzoxazol-2-yl)naphthol (L-5Me) and 3-(6-methylbenzoxazol-2-yl)naphthol (L-6Me) were synthesized as described earlier.[2] The C, H, N elemental analyses were performed by the Microanalytical laboratory of IOMC on Euro EA 3000 Elemental Analyser. The scandium and lanthanides content was analyzed by complexometric titration. IR spectra were obtained on a Perkin Elmer 577 spectrometer and recorded from 4000 to 450 cm^{-1} as a Nujol mull on KBr plates. The mass spectra were recorded on a Bruker Microflex LT mass spectrometer. The samples were excited at a wavelength of 337 nm at a maximum pulsed laser beam intensity of 150 μJ/pulse at 60 Hz. Absorption spectra were recorded on a UV/VIS instrument Perkin-Elmer Lambda-25 from 200 to 800 nm. Emission spectra were registered from 300 to 700 nm on a fluorescent spectrometer Perkin Elmer LS-55.

Synthesis of $Sc(L\text{-}5Me)_3$ (1)

A solution of 3-(5-methylbenzoxazol-2-yl)naphthol (119 mg, 0.432 mmol) in DME (10 ml) was added to a solution of $Sc[N(SiMe_3)_2]_3$ (76 mg, 0.14 mmol) in DME (5 ml). The reaction mixture was stirred for 30 min at room temperature. The precipitated small lemon-yellow crystals of **1** were separated by decantation, washed with cold DME and dried in vacuum. Yield 106 mg (85%). Anal. Calcd. (%) for $C_{54}H_{36}N_3O_6Sc$ (867.84): C, 74.74; H, 4.18; N, 4.84; Sc, 5.18. Found (%): C, 74.79; H, 4.24; N, 4.93; Sc, 5.14. IR (ν, cm^{-1}): 1627 (s), 1593 (s), 1523 (s), 1493 (m), 1377 (m), 1342 (s), 1310 (m), 1279 (m), 1263 (m), 1219 (w), 1191 (m), 1178 (m), 1146 (m), 1121 (w), 1046 (m), 1014 (w), 956 (w), 945 (w), 840 (m), 803 (m), 764 (m), 752 (s), 642 (m),.

The crystals of **1** suitable for X-ray analysis were obtained by slow cooling of warm (60°C) DME solution of the complex to room temperature.

Synthesis of Sc(L-6Me)$_3$ (2)

Complex **2** was prepared similarly to **1** from 3-(6-methylbenzoxazol-2-yl)naphthol (154 mg, 0.559 mmol) and Sc[N(SiMe$_3$)$_2$]$_3$ (98 mg, 0.186 mmol). Yield 140 mg (87%). Anal. Calcd. (%) for $C_{54}H_{36}N_3O_6Sc$ (867.84): C, 74.74; H, 4.18; N, 4.84; Sc, 5.18. Found (%): C, 74.69; H, 4.15; N, 4.80; Sc, 5.12. IR (ν, cm^{-1}): 1627 (s), 1607 (m), 1594 (m), 1524 (m), 1489 (m), 1378 (m), 1344 (s), 1330 (m), 1312 (w), 1279 (m), 1260 (w), 1219 (w), 1175 (m), 1145 (m), 1120 (w), 1040 (m), 922 (сл), 813 (m), 797 (m), 753 (s), 642 (w), 629 (w), 531 (s).

The crystals of **2** suitable for X-ray analysis were obtained by slow cooling of warm (60°C) DME solution of the complex to room temperature.

In a similar manner have been obtained the complexes:

Nd$_2$(L-5Me)$_6$ (3). From 3-(5-methylbenzoxazol-2-yl)naphthol (24 mg, 0.087 mmol) and Nd[N(SiMe$_3$)$_2$]$_3$ (18 mg, 0.029 mmol). Yield 24 mg (85%). Anal. Calcd. (%) for $C_{108}H_{72}N_6O_{12}Nd_2$ (1934.24): C, 67.06; H, 3.75; N, 4.34; Nd, 14.91. Found (%): C, 67.09; H, 3.85; N, 4.40; Nd, 14.97.

Nd$_2$(L-6Me)$_6$ (8). From 3-(6-methylbenzoxazol-2-yl)naphthol (87 mg, 0.320 mmol) and Nd[N(SiMe$_3$)$_2$]$_3$ (66 mg, 0.110 mmol). Yield 88 mg (86%). Anal. Calcd. (%) for $C_{108}H_{72}N_6O_{12}Nd_2$ (1934.24): C, 67.06; H, 3.75; N, 4.34; Nd, 14.91. Found (%): C, 67.03; H, 3.87; N, 4.43; Nd, 14.98.

Gd$_2$(L-5Me)$_6$ (4). From 3-(5-methylbenzoxazol-2-yl)naphthol (160 mg, 0.581 mmol) and Gd[N(SiMe$_3$)$_2$]$_3$ (124 mg, 0.194 mmol). Yield 162 mg (85%). Anal. Calcd. (%) for $C_{108}H_{72}N_6O_{12}Gd_2$ (1960.30): C, 66.17; H, 3.70; N, 4.29; Gd, 16.04. Found (%): C, 66.15; H, 3.67; N, 4.31; Gd, 16.07.

Gd$_2$(L-6Me)$_6$ (9). From 3-(6-methylbenzoxazol-2-yl)naphthol (110 mg, 0.400 mmol) and Gd[N(SiMe$_3$)$_2$]$_3$ (85 mg, 0.133 mmol). Yield 109 mg (83%). Anal. Calcd. (%) for $C_{108}H_{72}N_6O_{12}Nd_2$ (1960.30): C, 66.17; H, 3.70; N, 4.29; Gd, 16.04. Found (%): C, 66.19; H, 3.73; N, 4.27; Gd, 16.01.

Er$_2$(L-5Me)$_6$ (5). From 3-(5-methylbenzoxazol-2-yl)naphthol (176 mg, 0.639 mmol) and Er[N(SiMe$_3$)$_2$]$_3$ (138 mg, 0.213 mmol). Yield 180 mg (85%). Anal. Calcd. (%) for $C_{108}H_{72}N_6O_{12}Er_2$ (1980.28): C, 65.50; H, 3.66; N, 4.24; Er, 16.89. Found (%): C, 65.47; H, 3.62; N, 4.27; Er, 16.91.

Er$_2$(L-6Me)$_6$ (10). From 3-(6-methylbenzoxazol-2-yl)naphthol (98 mg, 0.356 mmol) and Er[N(SiMe$_3$)$_2$]$_3$ (77 mg, 0.119 mmol). Yield 100 mg (85%). Anal. Calcd. (%) for $C_{108}H_{72}N_6O_{12}Er_2$ (1980.28): C, 65.50; H, 3.66; N, 4.24; Er, 16.89. Found (%): C, 65.43; H, 3.65; N, 4.24; Er, 16.95;

$Tm_2(L\text{-}5Me)_6$ (6) From 3-(5-methylbenzoxazol-2-yl)naphthol (47 mg, 0.171 mmol) and $Tm[N(SiMe_3)_2]_3$ (37 mg, 0.057 mmol). Yield 49 mg (87%). Anal. Calcd. (%) for $C_{108}H_{72}N_6O_{12}Tm_2$ (1983.63): C, 65.39; H, 3.66; N, 4.24; Tm, 17.03. Found (%): C, 65.41; H, 3.68; N, 4.28; Tm, 16.97.

$Tm_2(L\text{-}6Me)_6$ (11) From 3-(6-methylbenzoxazol-2-yl)naphthol (39 mg, 0.141 mmol) and $Tm[N(SiMe_3)_2]_3$ (31 mg, 0.048 mmol). Yield 41 mg (87%). Anal. Calcd. (%) for $C_{108}H_{72}N_6O_{12}Tm_2$ (1983.63): C, 65.39; H, 3.66; N, 4.24; Tm, 17.03. Found (%): C, 65.44; H, 3.65; N, 4.26; Tm, 16.95.

$Yb_2(L\text{-}5Me)_6$ (7) From 3-(5-methylbenzoxazol-2-yl)naphthol (48 mg, 0.175 mmol) and $Yb[N(SiMe_3)_2]_3$ (38 mg, 0.058 mmol). Yield 50 mg (86%). Anal. Calcd. (%) for $C_{108}H_{72}N_6O_{12}Yb_2$ (1991.84): C, 65.12; H, 3.64; N, 4.22; Yb, 17.37. Found (%): C, 65.08; H, 3.61; N, 4.19; Yb, 17.40.

$Yb_2(L\text{-}6Me)_6$ (12). From 3-(6-methylbenzoxazol-2-yl)naphthol (120 mg, 0.436 mmol) and $Yb[N(SiMe_3)_2]_3$ (95 mg, 0.145 mmol). Yield 106 mg (73%). Anal. Calcd. (%) for $C_{108}H_{72}N_6O_{12}Yb_2$ (1991.84): C, 65.12; H, 3.64; N, 4.22; Yb, 17.37. Found (%): C, 65.05; H, 3.64; N, 4.16; Yb, 17.43.

The IR spectra of **3** - **7** are identical to that of **1**. The IR spectra of **8** - **12** are identical to that of **2**.

Device fabrication

The three-layer devices ITO/TPD (20 nm)/Ln-complex (50 nm)/BATH (20 nm)/Yb (150 nm), consisting of triphenyldiamine derivative (TPD) as a hole transport layer, 4,7-diphenyl-1,10-phenanthroline (BATH) as an electron-transporting and hole-blocking layer and the lanthanide complex as an emission layer, were fabricated in a vacuum chamber (10^{-6} mbar) with different resistive heaters for organic and metal layers. A commercial ITO on a glass substrate with 5 Ω/□ was used as the anode material (Luminescence Technology Corp.) and commercial Yb, 99.9% trace metals basis (Sigma-Aldrich) as the cathode material. The deposition rate for the organic compounds and Yb complex was 1 nm/s. The active area of the devices was 5×5 mm. The EL spectra and current-voltage-luminance characteristics were measured using an Ocean Optics USB-2000 fluorimeter, the computer controlled GW Instek PPE 3323 power supply and GW Instek GDM 8246 digital multimeter under ambient conditions.

X-ray Crystallographic Study

The X-ray data were collected on an Agilent Xcalibur E (for $Sc(L)_3$) and a Smart Apex diffractometer (for **1** and **2**) at T = 100(2) K. The structures were solved by direct methods and were refined on F^2 using *CrysAlis Pro*[3] ($Sc(L)_3$) and *SHELXTL*[4] (**1** and **2**) packages. All non-

hydrogen atoms were found from Fourier syntheses of electron density and were refined anisotropically. All hydrogen atoms were placed in calculated positions and were refined in the riding model (U_{iso}(H) = 1.5U_{eq}(C) in CH_3-groups and U_{iso}(H) = 1.2U_{eq}(C) in other groups). *ABSPACK (CrysAlis Pro)*[3] ($Sc(L)_3$) and *SADABS* [5] (**1** and **2**) were used to perform area-detector scaling and absorption corrections. The details of crystallographic, collection and refinement data are shown in Table S1 and corresponding cif files are available as supporting information. CCDC-993404 ($Sc(L)_3$), CCDC-993405 (**1**) and CCDC-993406 (**2**) contain the supplementary crystallographic data for this paper. These data can be obtained free of charge from The Cambridge Crystallographic Data Centre via ccdc.cam.ac.uk/products/csd/request/.

Table S1. Main crystallographic data and structure refinement details for $Sc(L)_3$, **1** and **2**

Complex	**$Sc(L)_3$**	**1**	**2**
Formula	$C_{55}H_{40}N_3O_7Sc$	$C_{58}H_{46}N_3O_{7.50}Sc$	$C_{58}H_{46}N_3O_8Sc$
M_r	899.86	949.94	957.94
crystal size, mm	0.3 x 0.1 x 0.1	0.22 x 0.16 x 0.06	0.22 x 0.19 x 0.16
Crystal system	Triclinic	Triclinic	Triclinic
Space group	P-1	P-1	P-1
a, Å	12.8021(2)	13.4946(18)	11.4280(6)
b, Å	13.4500(3)	13.5034(18)	14.9217(8)
c, Å	14.9393(3)	15.212(2)	15.1759(8)
α, º	85.2540(15)	114.329(3)	110.8230(10)
β, º	67.0451(17)	98.345(3)	95.9800(10)
γ, º	66.3028(18)	95.822(3)	98.0480(10)
V, Å^3	2160.58(8)	2458.8(6)	2361.6(2)
Z	2	2	2
$d_{calc.}$ g/cm^3	1.383	1.283	1.347
μ, mm^{-1}	0.232	0.208	0.218
F(000)	936	992	1000
θ,º	28.0	26.0	26.0
Reflections collected	38196	18466	20471
Reflections unique	10356	9415	9210
R_{int}	0.0603	0.0433	0.0252
R_1/wR_2 ($I > 2\sigma(I)$)	0.0470/0.0994	0.0752/0.1925	0.0571/0.1513
R_1/wR_2(all data)	0.0781/0.1082	0.1158/0.2093	0.0747/0.1627
$S(F^2)$	0.976	1.056	1.058
largest diff. peak and hole	0.361/-0.345	1.042/-0.500	1.622/-0.594

DFT study

The theoretical study of naphtolate complexes and free naphtoles were performed using the Density Functional Theory (DFT). Two approaches were applied: the hybrid B3LYP functional using DZVP basis set and the program Firefly 8.0),[6] which is partially based on the GAMESS (US)[7] source code and PBE functional with extended basis set H: (6s2p)/[2s1p], C,N,O:

(10s7p3d)/[3s2p1d], Sc: (19s,15p,11d,5f)/[6s,5p,3d,1f] implemented into Priroda program package;[8] Ln comlexes were treated in scalar-relativistic approximation, which is based on the full four-component one-electron Dirac equation with spin–orbit effects separated out.[9] The extended full four-component basis: Ln: (30s29p20d14f6g)/[9s8p6d3f1g], C,N,O: (10s7p3d)/[3s2p1d], H (6s,2p)/[2s1p] was used. This level of theory allows well to describe the coordination of ligands around Ln-center in contrast to nonrelativistic calculation with the extended basis set of the same quality using pseudopotential with inner shell relativistic effects included.[10] The optimized geometry of molecules was checked for the absence of imaginary frequencies. DFT/PBE quantum chemical calculations have been done using the facilities of Joint Supercomputer Center of the Russian Academy of Sciences.

The ground S_0 term and excited S_1-S_9 terms calculated using TD-DFT approach are shown in Fig. S1. The S_0-S_i transitions are distributed in the band width of 0.5 eV but differed greatly in their intensity. Only four of them are the same order of magnitude as that in the free HL ligand (corresponding S_i terms are shown by solid lines in Fig. S1). The intensity of the other transitions is one or two orders of magnitude smaller.

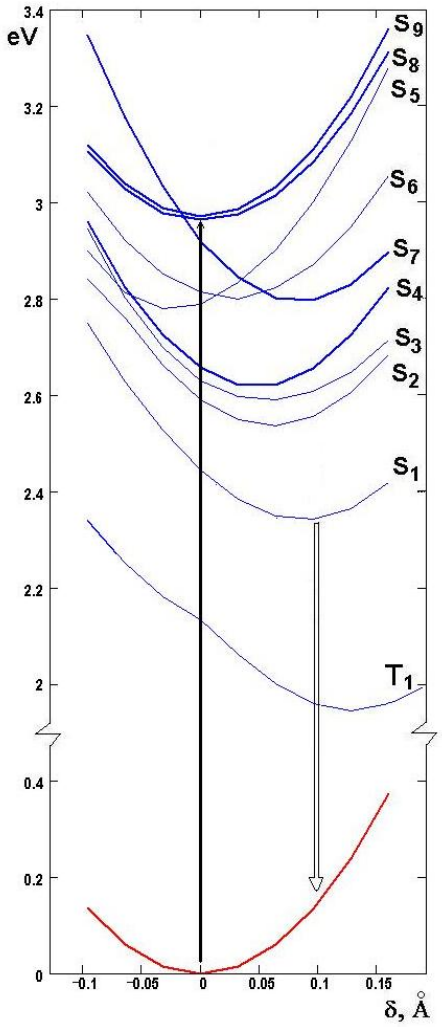

Fig. S1. The energy change of the ground and excited terms of the complex $Sc(L)_3$ in the transformation of its geometry in the direction to the equilibrium geometry of the lowest triplet state. The δ^2 value is the sum of squared variations of Sc-O and Sc-N distances along the geometry change. The energies of all the excited singlet terms are increased by 0.5 eV.

The geometry of binuclear complexes studied is similar to that of Nd_2L_6 complex.[11] Calculated geometry of this complex well corresponds to the experimental data. Although a mean deviation for Nd-O and Nd-N bonds is 0.02 Å, it is originated from different feature of terminal ligand coordination, with equivalent Nd-O in theoretical structure and equivalent Nd-N bonds in X-ray structure. So half of Nd-O and Nd-N distances have negligible deviations. The calculated structure of $Gd_2(L\text{-}6Me)_6$ complex is presented in the Fig. S2.

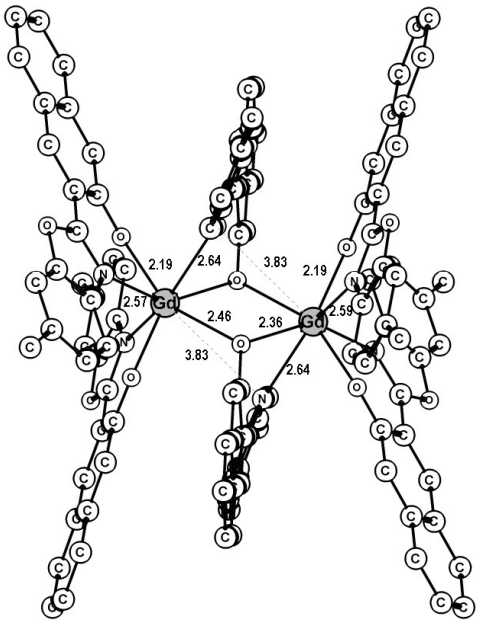

Fig. S2. Calculated molecular structure of binuclear complex $(L\text{-}6Me)_2$ Gd(μ-L-6Me)$_2$Gd(L-6Me)$_2$. Hydrogen atoms are omitted for clarity. The bond lengths are shown in Å.

The energies and oscillator strengths of S_0–S_n transitions were calculated in DFT/PBE approach with the time dependent density functional theory (TD-DFT) on the basis of structures optimized in their ground state S_0. The results are presented in the Table S2. The TD-DFT values have systematic error about 0.5 eV. Lowering of excited S terms is seen from the comparison of the energies of S_0–S_1, 1.94 eV, and S_0–T_1 2.14 eV transitions.

The absorption spectra for free LH ligand has only one low energy transition (λ_{max} 368 nm). So it is hard to explain the appearance of two low energy peaks in PL spectra of LH-6Me in THF solution (see Fig S3). But it was found that free ligands probably exist in form of dimers with energy release 3.5 kcal/mol. In the dimeric adduct four transitions in the band of 0.3 eV are

appear instead of one in solitary ligand. So, it is possible to assign these peaks to the S_4-S_0 transition with the highest oscillator strengths and to the lowest energy S_1-S_0 transition.

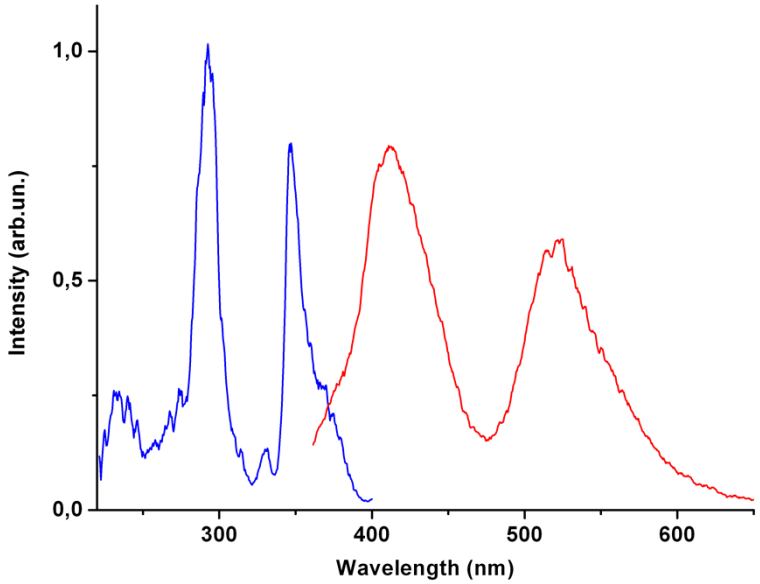

Fig. S3. Excitation (λ_{em} 412 nm) and PL (λ_{ex} 347 nm) spectra of LH-6Me ligand in THF solutions.

For the calculation of potential energy cross sections the geometry of S_1 state, which is hard to obtain, was approximated by the geometry of T_n state. In this state the main distortions, elongation and shortening of C-C bonds up to 0.04 Å, are observed in the ligand at the middle position with the largest Sc-N distance. Therefore value of total sum of all atomic displacements squared, $(0.82\ \text{Å})^2$, for $Sc(L)_3$ complex is much more than the total distortion of Sc coordination sphere, $Q^2 = (0.13\ \text{Å})^2$, where $Q^2 = \Sigma_i [\Delta R(Sc\text{-}L_i)]^2$, and $\Delta R(Sc\text{-}L_i)$ are values of differences of Sc-ligand distances in T_1 and S_0 states.

Table S2. Computed energies (TD-DFT/PBE) and Oscillator Strengths (f) for the Optical Transitions in $Sc(L)_3$ complex and in free ligand in Terms of Single Molecular Orbital Excitations

Transition number	MO contribution *	ΔE_{exp},eV	ΔE_{theor},eV	f
	$Sc(L)_3$ complex			
1	H → L , 1.00		1.94	0.0009
2	H → L+1 , 0.87		2.09	0.0035
3	H-1 → L , 0 .93		2.13	0.0009
4	H → L+2 , 0.72 H-1 → L+2 , -0.45		2.16	0.0122
5	H-2 → L+1 , 0.92		2.29	0.0018
6	H-2 → L+2 , 0.90		2.31	0.0135
7	H-1 → L+2 , 0.61 H → L+2 , 0.50 H-1 → L+1 , 0.50		2.42	0.0119
8	H-2 → L , 0 .69 H-1 → L+2 , 0.47 H-1 → L+1 , -0.41	2.95	2.46	0.0324
9	H-2 → L , 0 .57 H-1 → L+1 , 0.51		2.47	0.0208
17	H → L+4 , 0.66 H-1→ L+3 , -0.58	3.33	3.27	0.0144
21	H-5 → L , 0 .60 H-3 → L+2 , -0.33	3.56	3.37	0.2452
22	H → L+6 , 0.51 H-3 → L+2 , 0.43 H-4 → L+2 , 0.41	3.72	3.40	0.2308
23	H-6 → L , 0 .52 H → L+6 , -0.44	3.72	3.42	0.1888
25	H-6 → L , 0 .65 H-5 → L , -0.39	3.92	3.46	0.2422
	LH			
1	H → L , 0 .97		2.68	0.0254
2	H-1 → L , 0 .96		3.56	0.6734
	dimer $(LH)_2$			
1	H → L , 0 .86 H → L+1 , 0.47		2.47	0.0001
2	H-1 → L+1 , 0.85 H-1 → L -0.50		2.48	0.0001
3	H-1 → L , 0 .53 H → L+1 , 0.53 H-1→ L+1 , 0.44 H → L , -0.43		2.78	0.0058
4	H → L+1 , 0.65 H-1 → L , -0.64		2.78	0.0415
5	H-2 → L , 0 .64 H-3 → L , 0 .59		2.93	0.0001
6	H-2 → L+1 , 0.64 H-3 → L+1 , -0.59		2.93	0.0001
7	H-3 → L+1 , 0.66 H-2 → L , -0.65		3.51	0.0113
8	H-3 → L , 0 .65 H-2 → L+1 , -0.65	3.57	3.56	1.2192

* H≡HOMO, L≡LUMO. Only partial contribution larger than 0.4 are shown

(a)

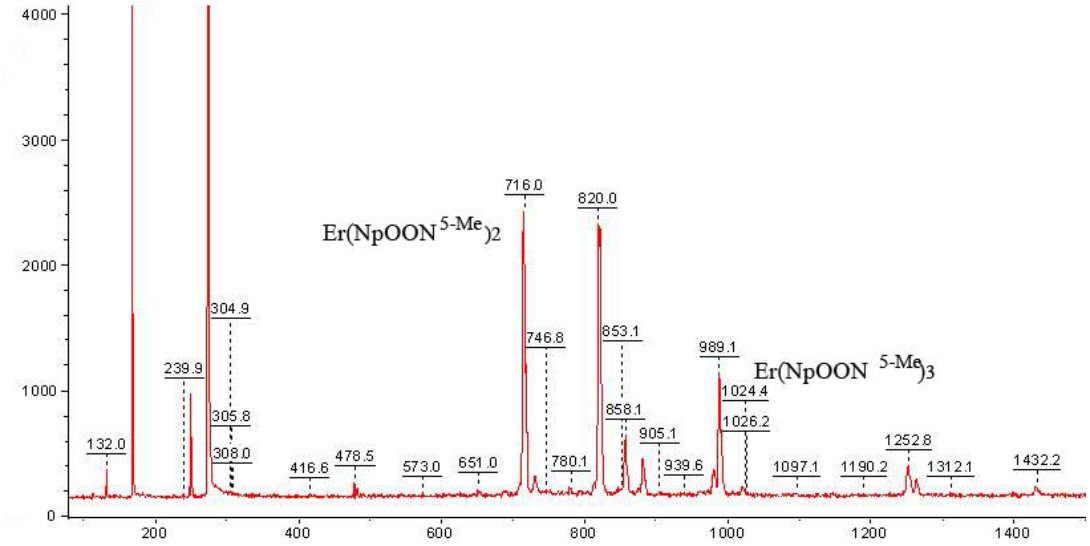

(b)

Fig. S4. Fragments of LDI-TOF spectra of the positive (a) and negative (b) ions of Er_2(L-5Me)$_6$ (**5**).

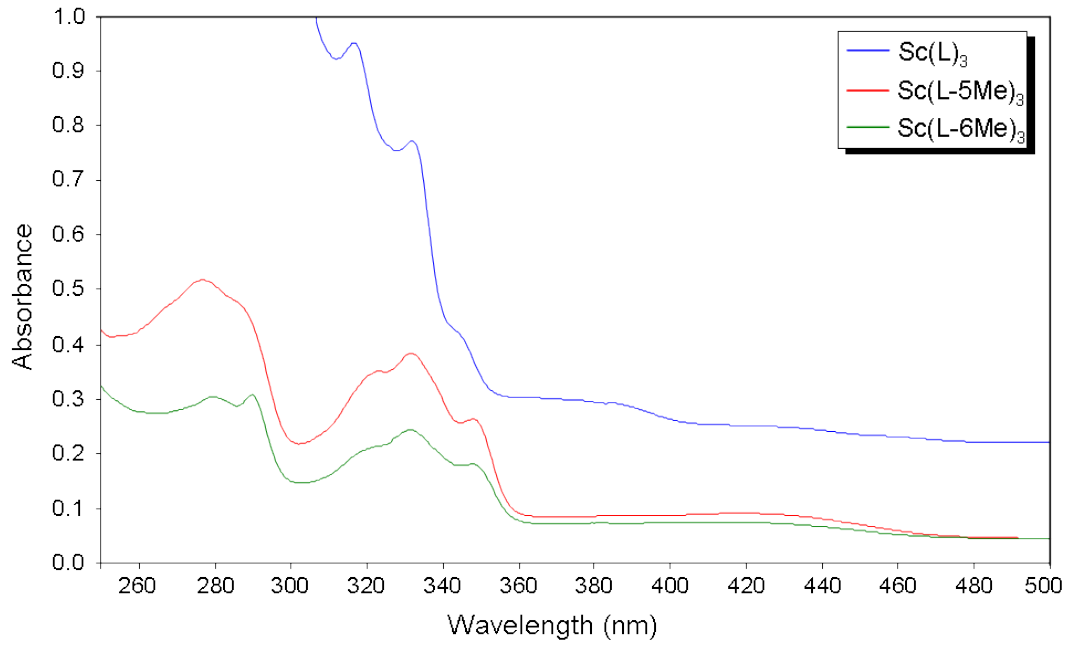

Fig. S5. Absorption spectra of scandium complexes Sc(L)$_3$, **1** and **2** in THF solutions.

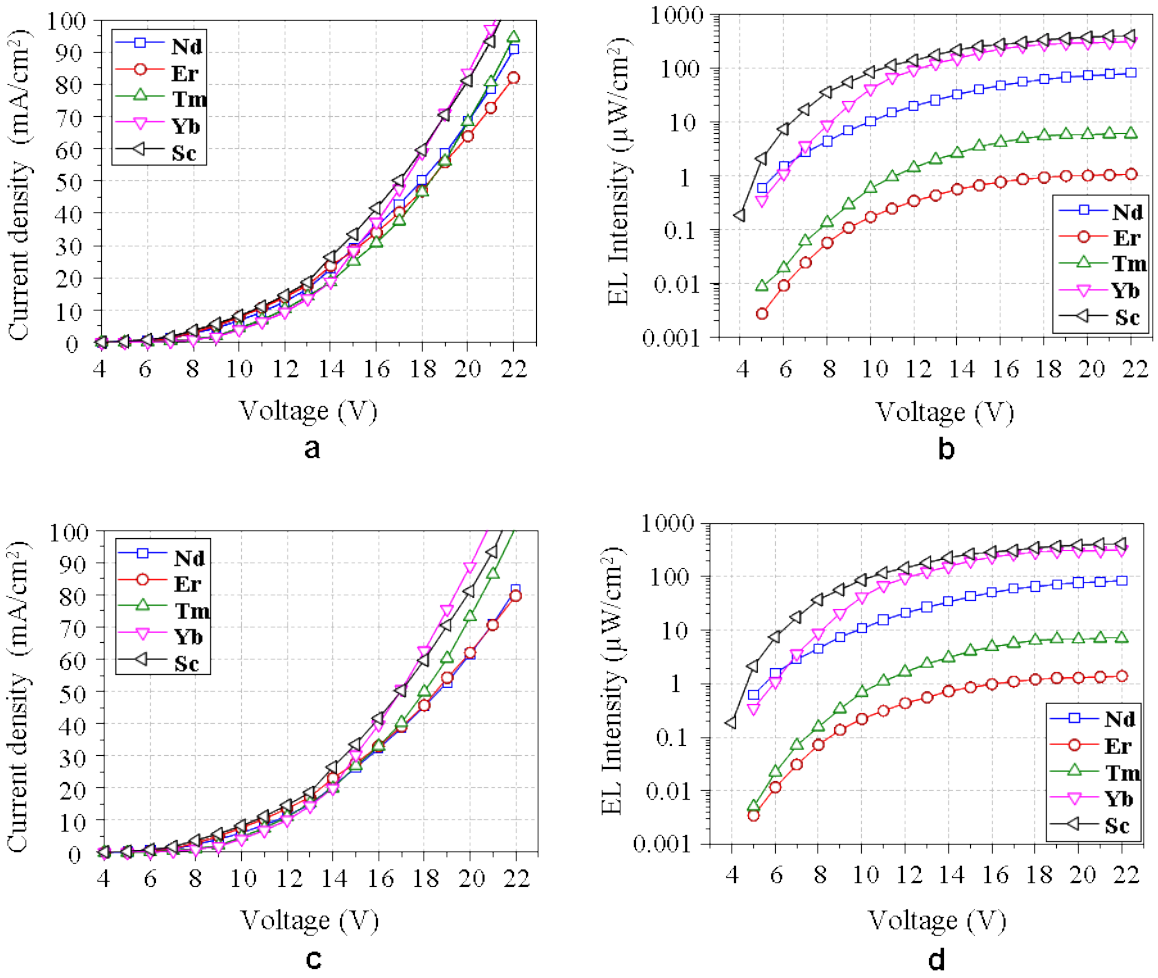

Fig. S6. Current-voltage and luminance-voltage of the devices based on **1**, **3**, **5-7** (a, b), **2**, **8**, **10 - 12** (c,d).

References

1. D. C. Bradley, J. S. Ghotra and F. A. Hart, *J. Chem. Soc. Dalt. Trans.,* 1973, **10**, 1021.

2. M. E. Burin, D. M. Kuzyaev, M. A. Lopatin, A. P. Pushkarev, V. A. Ilichev, D. L. Vorozhtsov, A. V. Dmitriev, D. A. Lypenko, E. I. Maltsev and M. N. Bochkarev, *Synth. Met.*, 2013, **164**, 55.

3. Agilent Technologies. CrysAlis Pro; Agilent Technologies Ltd, Yarnton, England, 2011.

4. G. M. Sheldrick, SHELXTL v.6.12, Structure Determination Software Suite, Bruker AXS, Madison, Wisconsin, USA, 2000.

5. G. M. Sheldrick, SADABS v.2.01, Bruker/Siemens Area Detector Absorption Correction Program, Bruker AXS, Madison, Wisconsin, USA, 1998.

6. A. A. Granovsky, Firefly version 8.0, www http://classic.chem.msu.su/gran/firefly/index.html.

7. M.W. Schmidt, K. K. Baldridge, J. A. Boatz, S. T. Elbert, M. S. Gordon, J. H. Jensen, S. Koseki, N. Matsunaga, K. A. Nguyen, S. Su, T. L. Windus, M. Dupuis and J. A. Montgomery, *J. Comput. Chem.*, 1993, **14**, 1347.

8. (a) D. N. Laikov, *Chem. Phys. Lett.*, 1997, **281**, 151; (b) D. N. Laikov, *Chem. Phys. Lett.*, 2005, **416**, 116.

9. K. G. Dyall, *J. Chem. Phys.*, 1994, **100**, 2118.

10. A. F. Shestakov and N. S. Emelyanova, *J. Mol. Structure: THEOCHEM* , 2010, **954**, 124.

11. A. P. Pushkarev, V. A. Ilichev, T. V. Balashova, D. L. Vorozhtsov, M. E. Burin, D. M. Kuzyaev, G. K. Fukin B. A. Andreev, D. I. Kryzhkov, A. N. Yablonskiy and M. N. Bochkarev, *Russ. Chem. Bull.* 2013**,** 395.